


High-pressure high-temperature synthesis and thermal equation of state of high-entropy transition metal boride ^F

Cite as: AIP Advances 11, 035107 (2021); <https://doi.org/10.1063/5.0045592>

Submitted: 28 January 2021 • Accepted: 11 February 2021 • Published Online: 03 March 2021

Seth Iwan,  Kaleb C. Burrage,  Bria C. Storr, et al.

COLLECTIONS

 This paper was selected as Featured



View Online



Export Citation



CrossMark

ARTICLES YOU MAY BE INTERESTED IN

[The emergent field of high entropy oxides: Design, prospects, challenges, and opportunities for tailoring material properties](#)

APL Materials 8, 040912 (2020); <https://doi.org/10.1063/5.0003149>

[Perspective: Superhard metal borides: A look forward](#)

APL Materials 6, 070901 (2018); <https://doi.org/10.1063/1.5040763>

[How high is the entropy in high entropy ceramics?](#)

Journal of Applied Physics 130, 150903 (2021); <https://doi.org/10.1063/5.0062523>



High-pressure high-temperature synthesis and thermal equation of state of high-entropy transition metal boride

Cite as: AIP Advances 11, 035107 (2021); doi: 10.1063/5.0045592

Submitted: 28 January 2021 • Accepted: 11 February 2021 •

Published Online: 3 March 2021



Seth Iwan,¹ Kaleb C. Burrage,¹  Bria C. Storr,¹  Shane A. Catledge,¹  Yogesh K. Vohra,^{1,a)} 
Rostislav Hrubíak,²  and Nenad Velisavljević³ 

AFFILIATIONS

¹Department of Physics, University of Alabama at Birmingham, Birmingham, Alabama 35294, USA

²High Pressure Collaborative Access Team (HPCAT), X-ray Science Division, Argonne National Laboratory, Argonne, Illinois 60439, USA

³HPCAT and Physics Division, Lawrence Livermore National Laboratory, Livermore, California 94550, USA

^{a)}Author to whom correspondence should be addressed: ykvohra@uab.edu

ABSTRACT

A high-entropy transition metal boride ($\text{Hf}_{0.2} \text{Ti}_{0.2} \text{Zr}_{0.2} \text{Ta}_{0.2} \text{Mo}_{0.2}$)B₂ sample was synthesized under high-pressure and high-temperature starting from ball-milled oxide precursors (HfO₂, TiO₂, ZrO₂, Ta₂O₅, and MoO₃) mixed with graphite and boron-carbide. Experiments were conducted in a large-volume Paris–Edinburgh press combined with *in situ* energy dispersive x-ray diffraction. The hexagonal AlB₂ phase with an ambient pressure volume $V_0 = 27.93 \pm 0.03 \text{ \AA}^3$ was synthesized at a pressure of 0.9 GPa and temperatures above 1373 K. High-pressure high-temperature studies on the synthesized high-entropy transition metal boride sample were performed up to 7.6 GPa and 1873 K. The thermal equation of state fitted to the experimental data resulted in an ambient pressure bulk-modulus $K_0 = 344 \pm 39 \text{ GPa}$, $dK/dT = -0.108 \pm 0.027 \text{ GPa/K}$, and a temperature dependent volumetric thermal expansion coefficient $\alpha = \alpha_0 + \alpha_1 T + \alpha_2 T^{-2}$. The thermal stability combined with a high bulk-modulus establishes this high-entropy transition metal boride as an ultrahard high-temperature ceramic material.

© 2021 Author(s). All article content, except where otherwise noted, is licensed under a Creative Commons Attribution (CC BY) license (<http://creativecommons.org/licenses/by/4.0/>). <https://doi.org/10.1063/5.0045592>

High-entropy materials containing a mixture of five or more elemental species represent a paradigm shift in materials science where a variety of oxides, carbides, and borides can be synthesized with superior physical and mechanical properties compared with those accessible from the constituent materials. In an endeavor to create ultrahard and high-temperature materials that retain their physical properties under extreme conditions, high entropy alloys (HEAs) have drawn considerable attention in recent years. Typically, alloys are made up of one base element with an addition of smaller ratios of secondary elements, and rarely are they made using more than two base elements.¹ HEAs, on the other hand, contain a random solid solution of five or more elements combined in equimolar ratios. The introduction of numerous elements that form into a singular metallic phase produces a large entropy of mixing, thereby lowering its Gibbs free energy and resulting in a stable high-entropy

material. The entropy of mixing $\Delta S_{\text{mix}} = R \ln(N)$, where R is the gas constant and N is the number of constituent elements. The large value of ΔS_{mix} ensures that high-entropy materials are stable at high temperatures and show a superior thermal degradation behavior under oxidizing environments.² Multiple HEAs have been discovered and studied^{3–5} with some elastic properties being notably better than those of their conventional alloy counterparts. The incorporation of boron into HEAs forms strong covalent bonds within the single metallic phase that further enhances the material strength in the new high entropy boride (HEB). This motivates the synthesis of HEB that is hard and thermally stable at 2000 K with physical properties similar to those seen in transition metal borides.^{6–11} Such a combination would pair a boride's alluring mechanical strength with an HEA's thermodynamic stability, producing a resilient material well suited for high temperature applications. In this paper, we report on

the synthesis of $(\text{Hf}_{0.2}\text{Ti}_{0.2}\text{Zr}_{0.2}\text{Ta}_{0.2}\text{Mo}_{0.2})\text{B}_2$ HEB starting from a powder mixture of HfO_2 , TiO_2 , ZrO_2 , Ta_2O_5 , MoO_3 , carbon black, and boron carbide. The HEB crystal structure was studied by Energy Dispersive X-ray Diffraction (EDXD) in a Paris–Edinburgh press, under quasi-hydrostatic pressure conditions, utilizing the setup at the Advanced Photon Source, High Pressure Collaborative Access Team (HPCAT) Beamline 16-BM-B, Argonne National Laboratory. We also established the thermal equation of state of the synthesized HEB material to 7.6 GPa and 1873 K and derived its thermoelastic properties.

The precursor materials contained equimolar amounts of five transition metal oxides— HfO_2 , TiO_2 , ZrO_2 , Ta_2O_5 , and MoO_3 —carbon black, and boron carbide, which were purchased from Alfa Aesar. First, the metal oxides combined with carbon are high energy ball milled (Spex 8000 M) for two hours in a tungsten carbide container and media. At hourly intervals, the ball mill is allowed to cool for 10 min. Boron carbide is then added to the mixture to blend by ball milling, with the milled metal oxides and carbon. To reduce contamination of tungsten carbide, the mixture with B_4C is wet milled in acetone for four hours with zirconia balls. The mixture includes an excess of B_4C (10%–15 wt. %) to account for the boron lost due to the formation of boron oxide and carbon monoxide, B_2O_3 and CO , during high pressure high temperature synthesis.¹² The milled mixture is left to dry in a vacuum oven before being passed through a 200-mesh sieve to ensure uniformity of particle size for subsequent processing.

High pressure–high temperature Energy Dispersive X-ray Diffraction (EDXD) experiments were conducted utilizing the white x-ray source and the Paris–Edinburgh press at the HPCAT beamline 16-BM-B. Data were collected with a diffraction angle $2\theta = 5^\circ$ and over an energy range of 5 KeV–120 KeV. The ball-milled sample mixture was compacted into cylinders of size 1 mm by 2 mm using a die press and placed within a boron nitride capsule, surrounded by a graphite heater, an MgO thermal insulating ring, a boron epoxy gasket, and a Lexan retaining ring. Two caps of ZrO_2 are placed on the top and bottom, along with tantalum rods and molybdenum foils, which provide the electrical conduction path from the tungsten carbide press anvils to the graphite heating element, as shown in Fig. 1.

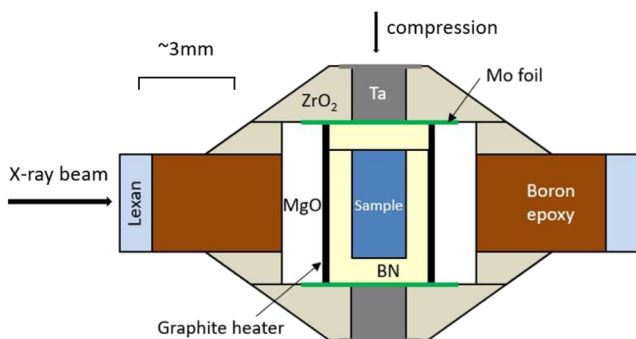


FIG. 1. Paris–Edinburgh cell and the sample assembly employed in the high-pressure high-temperature synthesis experiments at the HPCAT beamline 16-BM-B. The sample chamber contains a precursor mixture of metal oxides, graphite, and boron-carbide and was studied up to 7.6 GPa and 1873 K.

The temperature to power relationship was calibrated previously up to 2300 K as a function of applied pressure and measured with a W5%Re–W26%Re thermocouple in place of the sample.¹³ Sample pressure was estimated using the MgO pressure calibrant, which surrounds the sample and is shown in Fig. 1. *In situ* unit cell volumes of MgO were determined by EDXD, and pressure was calculated using the thermal equation of state formulated by Kono *et al.*¹⁴ The second order Birch–Murnaghan equation of state (BM EoS) in Eq. (1) was used with the Fei 1995 thermal expansion model^{15,16} shown in Eq. (2) to extract the bulk modulus (K_0), dK/dT , and the volumetric thermal expansion coefficient α ,

$$P(V) = \frac{3}{2}K_0 \left[x^{\frac{7}{3}} - x^{\frac{5}{3}} \right] \left[1 + \frac{3}{4}(K'_0 - 4)(x^{\frac{2}{3}} - 1) \right], \quad (1)$$

$$V_{0T} = V_{00} \exp \left(\alpha_0 (T - T_{ref}) + \frac{1}{2} \alpha_1 (T^2 - T_{ref}^2) + \alpha_2 \left(\frac{1}{T} - \frac{1}{T_{ref}} \right) \right). \quad (2)$$

In Eq. (1), $x = V_0/V$, K_0 is the bulk modulus, and K'_0 is the first pressure derivative. For Eq. (2), the temperature dependent volumetric thermal expansion α is described by coefficients α_0 , α_1 , α_2 as $\alpha = \alpha_0 + \alpha_1 T + \alpha_2 T^{-2}$. Some earlier published works^{17–19} employ a linear expansion to thermal expansion in Eq. (2) of the form $\alpha(T) = \alpha_0 + \alpha_1 T$. The linear term provides the lowest degree of estimation for temperature effects on expansion while the Fei model introduces a second order term with the added advantage that $\alpha(T)$ describes the volumetric change with temperature $\frac{1}{V_0T} \left(\frac{\partial V_0T}{\partial T} \right)$. The quadratic term is employed in this study for added accuracy in $\alpha(T)$ calculation in the high temperature range up to 1873 K. Temperature and pressure data were taken systematically by holding pressure constant and increasing temperature in 100 K steps up to the maximum temperature of 1973 K. The sample was then allowed to cool to ambient temperature before pressure was increased in ~ 0.5 GPa steps. In this manner, data of the thermal equation of state were generated on the high-entropy transition metal boride sample up to 7.6 GPa and 1873 K.

Figure 2 displays the EDXD data during heating to 1773 K at an average pressure of 0.9 GPa. The initial ambient temperature spectrum shows a mixture of HfO_2 , TiO_2 , ZrO_2 , Ta_2O_5 , and MoO_3 precursor phases mixed with graphite and boron-carbide, with particularly strong peaks between 2.5 Å and 3 Å for several overlapping phases. Synthesis of a new HEB is indicated by a gradual transformation beginning at 1373 K and progressing to completion to a hexagonal structure indicated by the appearance of three strong (101), (100), and (001) diffraction peaks of the AlB_2 hexagonal phase up to a maximum temperature of 1773 K. The indexed peaks of the hexagonal phase are shown in more detail in Fig. 3. The indexed nine diffraction peaks shown in Fig. 3 are used in the least square fit calculation of the interplanar d-spacing to calculate the lattice parameters, with values of $a = 3.14$ Å and $c = 3.43$ Å at 1973 K and 0.5 GPa. The residual graphite phase, boron carbide phase, and x-ray fluorescence lines from metal elements are also indicated. The (002) diffraction peak intensity from the residual graphite shown in Figs. 2 and 3 is unusually high and is attributed to preferred orientation effects as other reflections from graphite were not detected in the diffraction pattern. Our claim of equimolar composition of

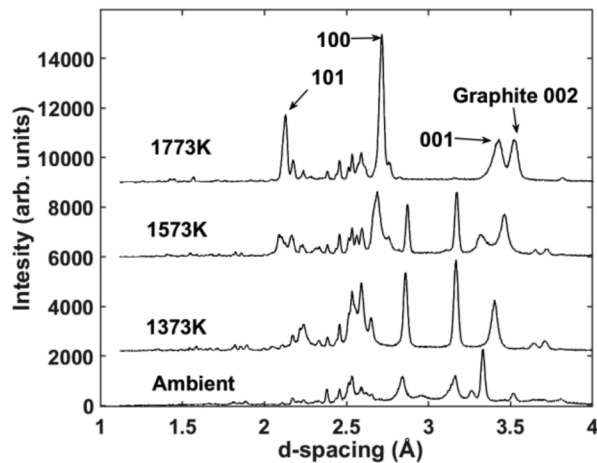


FIG. 2. Energy dispersive x-ray diffraction indicating the transformation of equimolar transition metal oxides (HfO_2 , TiO_2 , ZrO_2 , Ta_2O_5 , and MoO_3) into the HEB phase at an average pressure of 0.9 GPa. The HEB phase is characterized by the appearance of the three strong diffraction peaks (001), (100), and (101) from the hexagonal phase; a (002) residual peak from graphite is enhanced due to preferred orientation effects.

the synthesized HEB ($\text{Hf}_{0.2}\text{Ti}_{0.2}\text{Zr}_{0.2}\text{Ta}_{0.2}\text{Mo}_{0.2}\text{B}_2$) is supported by the initial equimolar composition of precursor metal oxides and the fact that we did not detect any residual metal oxides in x-ray diffraction after the high-temperature high pressure treatment, as shown in Fig. 3.

After synthesis, the new phase was shown to be stable when pressure and temperature were relaxed to ambient conditions. Further heating and compression cycles showed the stability of the synthesized AlB_2 phase to 7.6 GPa and 1973 K. Thermodynamic stability is one of the hallmarks of this class of HEB as the high entropy provides phase stability at high temperatures and a possible retention of high hardness at high temperatures.² Figure 4 shows our P-V-T data on the HEB sample up to 7.6 GPa and 1873 K. The data of measured thermal equation of state were fitted to Eqs. (1)

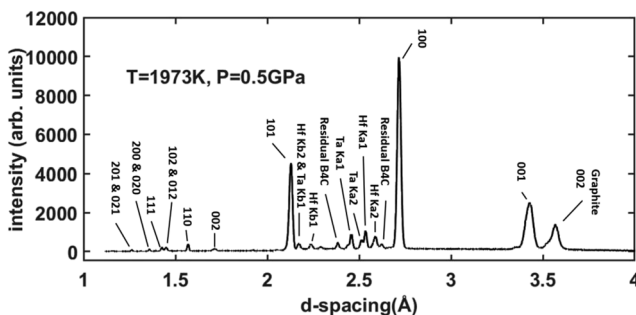


FIG. 3. Detailed assignment of diffraction and sample fluorescence peaks at 0.5 GPa and 1973 K. There are nine-diffraction peaks attributed to the hexagonal AlB_2 phase of the HEB sample while the weak peaks from the residual graphite and the B_4C phase are also indicated. The single diffraction peak from the residual graphite is enhanced due to orientation effects.

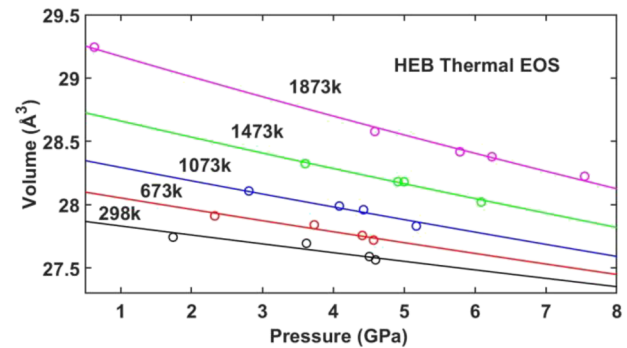


FIG. 4. Measured P-V-T for the synthesized HEB sample up to 7.6 GPa and 1873 K.

and (2), and the elastic and thermal properties were derived from the measured data.

The fits to P-V-T data shown in Fig. 4 yield information on the thermoelastic properties of the synthesized HEB sample. The fits resulted in an ambient pressure volume $V_0 = 27.93 \pm 0.03 \text{ Å}^3$ and the bulk modulus $K_0 = 344 \pm 39 \text{ GPa}$ at ambient temperature with a fixed value of $K'_0 = 4$. The fitted value of the temperature derivative of the bulk modulus is $dK/dT = -0.108 \pm 0.027 \text{ GPa/K}$. Thermal expansion coefficients were calculated using the Fei 1995 temperature modification and shown to be $\alpha_0 = -1.10 \times 10^{-5} \text{ K}^{-1}$, $\alpha_1 = 3.40 \times 10^{-8} \text{ K}^{-2}$, and $\alpha_2 = 2.97 \text{ K}$ with the volumetric thermal expansion expressed as $\alpha = \alpha_0 + \alpha_1 T + \alpha_2 T^{-2}$ in the temperature range between 300 K and 2000 K.

We have successfully synthesized a high-entropy transition metal boride sample ($\text{Hf}_{0.2}\text{Ti}_{0.2}\text{Zr}_{0.2}\text{Ta}_{0.2}\text{Mo}_{0.2}\text{B}_2$) from the precursor oxide materials HfO_2 , TiO_2 , ZrO_2 , Ta_2O_5 , and MoO_3 mixed with carbon black and boron carbide under high-pressures and high-temperatures. The synthesis was carried out at a pressure of 0.9 GPa and temperatures above 1373 K, and the sample was shown to be a hexagonal AlB_2 structure with ambient conditions volume $V_0 = 27.93 \pm 0.03 \text{ Å}^3$. A bulk modulus of $K_0 = 344 \pm 39 \text{ GPa}$ was derived from the measured equation of state at ambient temperature along with $dK/dT = -0.108 \pm 0.027 \text{ GPa/K}$. The thermal volume expansion coefficient in the temperature range between 300 K and 2000 K is described by $\alpha = \alpha_0 + \alpha_1 T + \alpha_2 T^{-2}$, with $\alpha_0 = -1.10 \times 10^{-5} \text{ K}^{-1}$, $\alpha_1 = 3.40 \times 10^{-8} \text{ K}^{-2}$, and $\alpha_2 = 2.97 \text{ K}$. Our studies indicate that the hexagonal AlB_2 phase of the synthesized ($\text{Hf}_{0.2}\text{Ti}_{0.2}\text{Zr}_{0.2}\text{Ta}_{0.2}\text{Mo}_{0.2}\text{B}_2$) material is stable up to 7.6 GPa and 1873 K, thereby establishing high-entropy transition metal boride as a promising ultrahard high temperature ceramic material.

This material was based on work supported by the Department of Energy-National Nuclear Security Administration, under Award No. DE-NA0003916. S.I. would like to acknowledge the Graduate Fellowship support under the NASA/Alabama Space Grant Consortium, Grant No. NNN19ZHA001C. Portions of this work were performed at the HPCAT (Sector 16), Advanced Photon Source (APS), Argonne National Laboratory. HPCAT operations are supported by DOE-NSA's Office of Experimental Sciences. The Advanced Photon Source is a U.S. Department of Energy (DOE) Office of Science

User Facility operated for the DOE Office of Science by Argonne National Laboratory, under Contract No. DE-AC02-06CH11357. The work of N.V. was performed under the auspices of the U.S. Department of Energy by Lawrence Livermore National Laboratory under Contract No. DE-AC52-07NA27344.

DATA AVAILABILITY

The data that support the findings of this study are available from the corresponding author upon reasonable request.

REFERENCES

- ¹E. P. George, D. Raabe, and R. O. Ritchie, "High-entropy alloys," *Nat. Rev. Mater.* **4**, 515 (2019).
- ²J. Gild, Y. Zhang, T. Harrington, S. Jiang, T. Hu, M. C. Quinn, W. M. Mellor, N. Zhou, K. Vecchio, and J. Luo, "High-entropy metal diborides: A new class of high-entropy materials and a new type of ultrahigh temperature ceramics," *Sci. Rep.* **6**, 37946 (2016).
- ³Y. Zhang, T. T. Zuo, Z. Tang, M. C. Gao, K. A. Dahmen, P. K. Liaw, and Z. P. Lu, "Microstructures and properties of high-entropy alloys," *Prog. Mater. Sci.* **61**, 1 (2014).
- ⁴N. Ishizu and J. Kitagawa, "New high-entropy alloy superconductor $\text{Hf}_{21}\text{Nb}_{25}\text{Ti}_{15}\text{V}_{15}\text{Zr}_{24}$," *Results Phys.* **13**, 102275 (2019).
- ⁵B. Gludovatz, A. Hohenwarter, D. Catoor, E. H. Chang, E. P. George, and R. O. Ritchie, "A fracture-resistant high-entropy alloy for cryogenic applications," *Science* **345**(6201), 1153–1158 (2014).
- ⁶A. Erdogan, A. Günen, M. S. Gök, and S. Zeytin, "Microstructure and mechanical properties of borided $\text{CoCrFeNiAl}_{0.25}\text{Ti}_{0.5}$ high entropy alloy produced by powder metallurgy," *Vacuum* **183**, 109820 (2020).
- ⁷H.-Y. Chung, M. B. Weinberger, J. B. Levine, A. Kavner, J.-M. Yang, S. H. Tolbert, and R. B. Kaner, "Synthesis of ultra-incompressible superhard rhenium diboride at ambient pressure," *Science* **316**, 436 (2007).
- ⁸M. Frotscher, A. Senyshyn, and B. Albert, "Neutron diffraction at metal borides, Ru_2B_3 and Os_2B_3 ," *Z. Anorg. Allg. Chem.* **638**, 2078 (2012).
- ⁹K. C. Burrage, C.-M. Lin, W.-C. Chen *et al.*, "Experimental and computational studies on superhard material rhenium diboride under ultrahigh pressures," *Materials* **13**, 1657 (2020).
- ¹⁰A. Kavner *et al.*, "Thermoelastic properties of ReB_2 at high pressures and temperatures and comparison with Pt, Os, and Re," *J. Appl. Phys.* **110**, 093518 (2011).
- ¹¹A. Friedrich *et al.*, "Synthesis of binary transition metal nitrides, carbides and borides from the elements in the laser-heated diamond anvil cell and their structure-property relations," *Materials* **4**, 1648 (2011).
- ¹²L. Feng, W. G. Fahrenholtz, and G. E. Hilmas, "Two-step synthesis process for high-entropy diboride powders," *J. Am. Ceram. Soc.* **103**(2), 724 (2019).
- ¹³Y. Kono, C. Park, C. Kenney-Benson, G. Shen, and Y. Wang, "Toward comprehensive studies of liquids at high pressures and high temperatures: Combined structure, elastic wave velocity, and viscosity measurements in the Paris-Edinburgh cell," *Phys. Earth Planet. Inter.* **228**, 269 (2014).
- ¹⁴Y. Kono, T. Irifune, Y. Higo, T. Inoue, and A. Barnhoorn, "PVT relation of MgO derived by simultaneous elastic wave velocity and in situ X-ray measurements: A new pressure scale for the mantle transition region," *Phys. Earth Planet. Inter.* **183**, 196 (2010).
- ¹⁵Y. Fei, "Thermal expansion," in *Mineral Physics & Crystallography* (American Geophysical Union (AGU), 2013), pp. 29–44.
- ¹⁶O. L. Anderson, *Equations of State of Solids for Geophysics and Ceramic Science* (Oxford University Press, Oxford, UK, 1995).
- ¹⁷J. Zhang and P. Kostak, "Thermal equation of state of magnesiowüstite ($\text{Mg}_{0.6}\text{Fe}_{0.4}\text{O}$)," *Phys. Earth Planet. Inter.* **129**, 301 (2002).
- ¹⁸Y. Wang, J. Zhang, H. Xu, Z. Lin, L. L. Daemen, Y. Zhao, and L. Wang, "Thermal equation of state of copper studied by high P-T synchrotron X-ray diffraction," *Appl. Phys. Lett.* **94**, 071904 (2009).
- ¹⁹Y. Wang, Z. T. Y. Liu, S. V. Khare, S. A. Collins, J. Zhang, L. Wang, and Y. Zhao, "Thermal equation of state of silicon carbide," *Appl. Phys. Lett.* **108**, 061906 (2016).